



PAWEŁ TCHÓRZEWSKI

Netrix S.A., Poland

ORCID iD: orcid.org/0000-0001-8344-8828

MALGORZATA LALAK-DYBAŁA

WSEI University in Lublin, Poland

ORCID iD: orcid.org/0000-0001-5694-3460

BARTOSZ PRZYSUCHA

Lublin University of Technology, Poland

ORCID iD: orcid.org/0000-0002-1117-8088

PAWEŁ OLSZEWSKI

WSEI University in Lublin, Poland

ORCID iD: orcid.org/0000-0002-1015-1190

USE OF ELECTRICAL IMPEDANCE TOMOGRAPHY FOR LUNG VOLUME RECONSTRUCTION

ZASTOSOWANIE ELEKTRYCZNEJ TOMOGRAFII IMPEDANCYJNEJ DO REKONSTRUKCJI OBJĘTOŚCI PŁUC

ABSTRACT

The article presents a study of the application of electro-impedance tomography (EIT) in diagnosing lung capacity using the Tikhonov regularization method. The possibility of reconstructing the lungs to monitor the degree of air filling was investigated. The experiment included a series of tests using a torso phantom designed to simulate different states of the lungs – from fully inflated to fully deflated. Lung-filling states were manipulated in controlled scenarios to test nine main experimental conditions reflecting different lung-filling states. In addition, the quality of reconstruction was checked using various types of reference backgrounds. The results show significant differences in lung volume reconstructions depending on the lung filling state. The most successful reconstructions, which were obtained using the 'No phantom' background, provided the most explicit visualization of the lungs, reassuring the method's reliability. The experiments confirm the potential of EIT to distinguish between different lung states and reconstruct the degree of lung filling. The study also underscores the need to optimize the reference background to increase the precision of the images, especially for the left lung.

STRESZCZENIE

Artykuł przedstawia badania zastosowania elektroimpedancyjnej tomografii (EIT) w diagnostyce pojemności płuc za pomocą metody regularyzacji Tichonowa. Zbadano możliwości rekonstrukcji płuc w celu monitorowania stopnia ich wypełnienia powietrzem. Eksperyment objął serię testów z użyciem fantomu klatki piersiowej, zaprojektowanego do symulacji różnych stanów płuc – od całkowicie napełnionych do całkowicie opróżnionych. Manipulowano stanami wypełnienia płuc w kontrolowanych scenariuszach, aby zbadać dziewięć głównych warunków eksperymentalnych odzwierciedlających różne stany wypełnienia płuc. Dodatkowo sprawdzono jakość rekonstrukcji przy wykorzystaniu różnych rodzajów tła referencyjnego. Wyniki wskazują na znaczące różnice w rekonstrukcjach objętości płuc, zależne od stanu ich wypełnienia. Najskuteczniejsze rekonstrukcje uzyskano przy użyciu tła 'No phantom', które zapewniło najwyraźniejszą wizualizację płuc. Eksperymenty potwierdzają potencjał EIT do rozróżniania różnych stanów płuc oraz rekonstrukcji stopnia ich wypełnienia. Badanie podkreśla również potrzebę optymalizacji tła referencyjnego w celu zwiększenia precyzji obrazów, zwłaszcza dla lewego płuca.

KEYWORDS: *Electrical impedance tomography, lung volume reconstruction, pulmonary diagnostics, medical imaging, phantom examination*

SŁOWA KLUCZOWE: *elektryczna tomografia impedancyjnej, rekonstrukcja objętości płuc, diagnostyka pulmonologiczna, obrazowanie medyczne, badanie fantomowe*

INTRODUCTION

Tomography is an imaging technique used in medicine and industry that allows detailed visualization of the internal structure of objects or organisms under study without opening or destroying them. Tomographic techniques are divided into invasive and non-invasive, with different applications depending on the accuracy and resolution of the images needed.

Invasive methods, such as angiography and endoscopy, require surgical intervention or the insertion of instruments into the body. Angiography, which involves the introduction of a contrast agent into the blood vessels, is crucial in diagnosing cardiovascular disease (Omeh and Shlofmitz, 2023). Endoscopy, which allows direct visualization of the inside of organs, is widely used in analyzing the stomach or intestines (The et al., 2020). Computed tomography (CT), using X-rays, is used to diagnose trauma, cancer, and circulatory problems thanks to its ability to produce cross-sectional images of the body (Morigi et al., 2022).

Non-invasive methods such as magnetic resonance imaging (MRI) and ultrasound (USG) are valuable for their safety and speed of image acquisition. MRI uses strong magnetic fields and radio waves to generate detailed images of soft tissues (Mikulka, 2015; Kak and Slaney, 1999; Zywica et al., 2020), while ultrasound, using high-frequency sound waves, helps monitor pregnancy and internal organ function, although its image quality can be limited (Mojabi and Vetri, 2016; Wiskin et al., 2020). Electroimpedance tomography (EIT), based on measuring changes in tissue electrical conductivity, is used both in medicine to monitor lung and heart function (Mansouri et al.2021) and in industry to analyze material properties (Garbaa et al., 2016; Banasiak, 2014; Kryszyn and Smolik, 2017; Kryszyn and Wanta, 2017, Majchrowicz et al., 2017; Wajman et al., 2013). Optical tomography, including techniques like optical coherence tomography (OCT), offers high-resolution images of tissue surfaces, particularly useful in ophthalmology and dermatology but with limited penetration depth. In industry, computed tomography (CT) is used for quality control, inspection of machine components, and detection of internal defects without destroying the product (Rymarczyk and Kłosowski 2019; Wang et al. 2010; Garbaa et al. 2016.; Rymarczyk et al. 2021). These techniques also allow for material analysis, such as detecting

wall moisture (Rymarczyk et al., 2018; Berowski et al., 2005). or leaks in the floodwalls (Kłosowski et al., 2018; Rymarczyk et al., 2021).

Electrical impedance tomography (EIT) is a non-invasive imaging method that is increasingly used in clinical medicine, primarily to monitor lung or cardiac function. The process is based on measuring changes in tissue electrical conductivity induced by externally applied currents of low intensity and frequency. The recorded changes are analyzed and transformed into images that provide valuable diagnostic and monitoring information. EIT allows observation of dynamic physiological processes in real-time, without harmful radiation, which is a significant advantage, especially in intensive care and monitoring of critical conditions (Mansouri et al., 2021).

The importance of EIT is particularly significant in assessing the condition of the lungs, where traditional methods such as chest X-rays and CT scans may be inadequate due to their invasiveness or radiation exposure. The ability to advance this technology to provide real-time information will allow physicians to continuously track lung and heart function, which is crucial in cases such as acute lung injury or chronic obstructive pulmonary disease. This article aims to present detailed findings on using EIT for the torso phantom, highlighting the potential of this method to improve lung monitoring. The paper also investigates the challenges of implementing this technology in real-world clinical trials and its future medical applications.

RESEARCH METHODOLOGY

The inverse problem is a critical issue in the reconstruction of CT images. In solving the inverse problem in tomography, both deterministic methods, such as the integer variable method (Xi, 2020), Gauss-Newton algorithm with Tikhonov penalization (Bangti and Maass, 2012), and machine learning methods, including neural networks (Kłosowski et al., 2021), elastic net method (Rymarczyk and Kłosowski, 2019) or logistic regression (Rymarczyk et al. 2021), are used. A comparison of the quality of reconstruction using different methods can be found in the literature (Rymarczyk et al. 2021; Kłosowski et al. 2021).

In this study, the Gauss-Newton algorithm was used to reconstruct images. This algorithm is notably recognized for its effectiveness in improving image quality while minimizing the impact of noise. In electro-impedance tomography, image reconstruction based on potential measurements at the body surface is an inherently poorly conditioned problem, meaning that even small changes in the input data can lead to significant differences in the results. In this context, using appropriate methods to stabilize the solution becomes crucial. One of the most effective approaches for tackling ill-conditioned problems is Tikhonov regularization. This method significantly improves image reconstruction quality by adding a regularization factor, otherwise known as a penalty, to the inversion problem. Thus, the Tikhonov algorithm effectively stabilizes solving the inverse problem. In Tikhonov's algorithm, the objective function given by equation (1) must be minimized.

$$F(\boldsymbol{\gamma}) = \frac{1}{2} \left\{ \|\mathbf{L}_1 (\mathbf{U}_m - \mathbf{U}_s(\boldsymbol{\gamma}))\|^2 + \lambda^2 \|\mathbf{L}_2 (\boldsymbol{\gamma} - \boldsymbol{\gamma}^*)\|^2 \right\} \quad (1)$$

$\boldsymbol{\gamma}$ – conductivity vector, $\boldsymbol{\gamma}^*$ – the a priori assumed conductivity vector, U_m – voltage measured experimentally, $U_s(\boldsymbol{\gamma})$ – voltage calculated using numerical methods (FEM), L_1, L_2 – regularization matrix, λ – regularization parameter.

The experiment used a torso phantom, which allowed controlled simulations of physiological conditions necessary to evaluate the algorithm's effectiveness under realistic but stable laboratory conditions.

TORSO PHANTOM

The torso phantom created for the study was designed as a simplified version of the lungs. It preserves the original overall shape of the natural lungs. By omitting more complex structures and details, it is possible to test the reproducibility of the images on the one hand and create a simplified model for subsequent modifications on the other. The model was designed to reproduce the asymmetry of natural lungs – the right lung is larger than the left lung, corresponding to the natural arrangement of organs to make room for the

heart Figure 1. The model's height can be adjusted, and electrode mounts were installed at shoulder height. The phantom was constructed with multiple gluing steps to increase its strength and tightness.

Figure 1. *Photo of the Phantom and measurement system*



Graphite electrodes with a diameter of 4 mm were attached to the phantom, placed on laminated copper tapes, and secured with plastic sleeves. These electrodes are connected to PCBs that contain SMB sockets and mounted on the aforementioned tapes. Each electrode is part of a complete mounting system, which allows easy placement around the phantom circuit.

In addition, for the study of lung function, the trachea was mapped using a tube through which air was pumped. Such a procedure allows disturbances resulting from the trachea and the patient's breathing to be introduced into the measurements. The device is powered by an external 12V/2A DC voltage source and controlled by a PWM controller, which allows the speed of air pumping to be adjusted.

FINITE ELEMENT METHOD

The finite element method was used to model the torso phantom. The finite element method (FEM) for impedance tomography (EIT) involves a three-dimensional space analysis for this study, with a quadrilateral finite element mesh model (Kania et al. 2022).

One then considers the functional in the space of three-dimensional form:

$$E(\phi) = \iint_{\Pi} \int_{\Omega} \sigma \|\nabla \phi(v)\|^2 d\pi + \sum_l \frac{1}{z_l} \int_{\Omega} (\phi - U_l)^2 d\omega \quad (2)$$

The solution of the simple problem reduces to the minimization of the above function, where zero variation is necessary for minimization.

$$\delta E(\phi) = 2 \int_{\Pi} \sigma \nabla \phi(v) \cdot \nabla (\delta \phi) dv + \sum_l \frac{2}{z_l} \int_{\Omega} (\phi - U_l) \delta \phi d\omega = 0 \quad (3)$$

where $\nabla \phi(v)$ – electric potential gradient ϕ , $d\pi$ – volume element, $d\omega$ – surface component, σ – electrical conductivity, U_l – electrical potential on electrodes, $\delta \phi$ – variance of potential, z_l – coefficient characterizing the electrodes, Ω – volume area, Π – the surface on which the electrodes are placed.

The primary goal of FEM in EIT is to solve the above functions by discretizing the analysis area into smaller manageable units (finite elements), using interpolating functions that allow approximation of the potential distribution in the analyzed area. This method allows efficient solutions to engineering and medical problems, such as reconstruction of images of internal body structures.

For finite elements in the form of tetrahedrons, the final sensitivity matrix is obtained using equations (4) and (5).

$$MS = -\frac{1}{I} \int_{\Omega} \nabla \phi \cdot \nabla \psi d\Omega, \quad (4)$$

$$MS = -\frac{1}{I} \int_{\Omega} \frac{\partial \phi}{\partial x} \frac{\partial \psi}{\partial x} + \frac{\partial \phi}{\partial y} \frac{\partial \psi}{\partial y} + \frac{\partial \phi}{\partial z} \frac{\partial \psi}{\partial z} dx dy dz \quad (5)$$

where, ϕ is the potential at the nodes for electrode stimulation, while the ψ is the potential at the nodes for the measuring electrodes.

The sensitivity matrix is key to determining how changes in conductivity affect measured voltages in EIT. It expresses the linear relationship between small changes in conductivity and induced changes in electrode voltages.

RESULTS

The experiment involved analyzing the ability to reconstruct lung capacity using an advanced imaging technique. The study involved a series of experiments in which the lung-filling state was manipulated in different configurations. Various states of both lungs were tested, from fully blown to fully inflated, in different combinations for each lung. Nine central experimental states were created, described as other states of lung filling: from full expiration (both lungs blown out) through intermediate states to full inspiration (both lungs filled with air).

In addition, the experiment included three different reference backgrounds: 'No phantom,' 'Background Lungs,' and 'Background Spine.' Changing the reference background was intended to investigate how different backgrounds affect the visibility and reconstruction of the lungs during the imaging process.

Figure 2. Case reconstructions: Left lung in an intermediate state, right lung filled
 a)reference ,No phantom', b)reference ,Background Lungs', c)reference ,Background Spine'
 d)photo of phantom

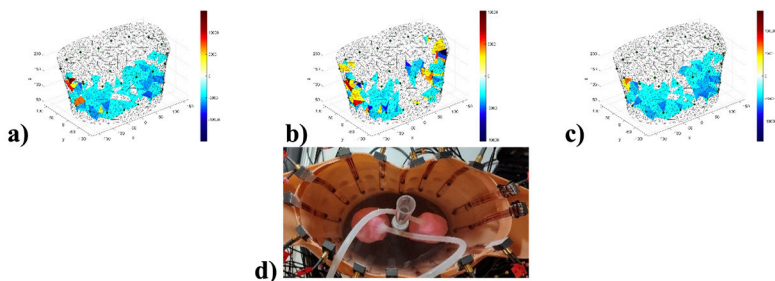


Figure 3. Case reconstructions: Left lung in intermediate state, right lung pumped out (a) reference 'Without phantom', (b) reference 'Lungs in background', (c) reference 'Spine in background' (d) photo of phantom

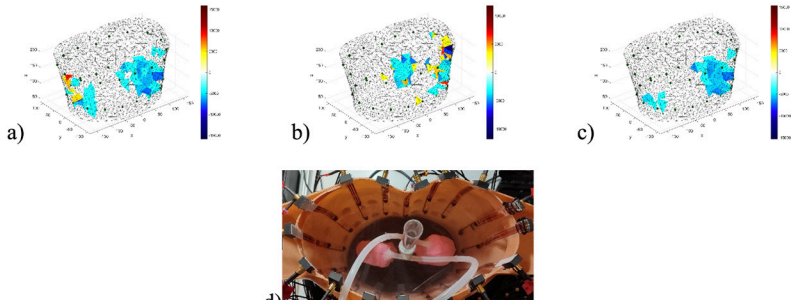


Figure 4. Case reconstructions: The left lung is filled, and the right lung is in an intermediate state (a) reference No phantom, (b) reference Lungs in the background, (c) reference Spine in the background (d) photo of the phantom

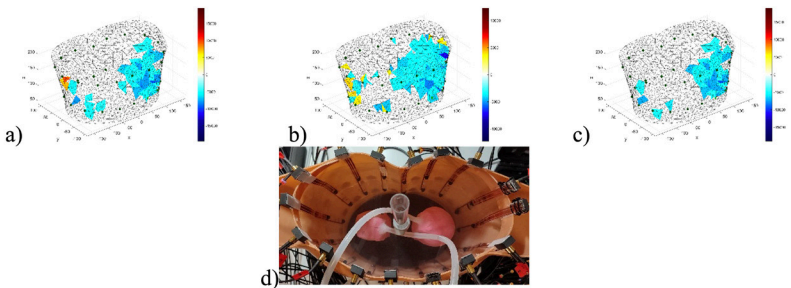


Figure 5. Case reconstructions: Left lung is wholly filled, the right lung is pumped out (a) reference 'Without phantom', (b) reference 'Lungs in the background', (c) reference 'Spine in background' (d) photo of phantom

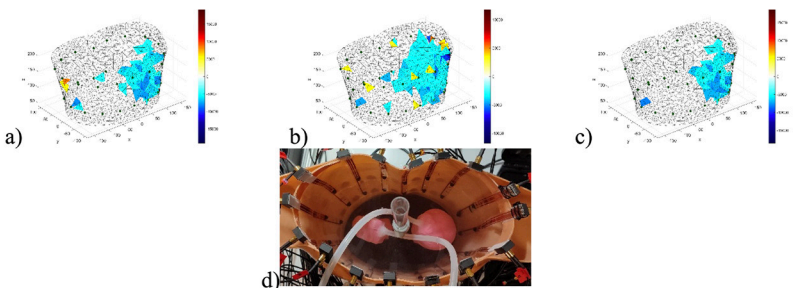


Figure 6. Case reconstructions: The left lung is pumped out, and the right lung is in an intermediate state a) Reference 'Without phantom', b) Reference 'Lungs in the background', c) Reference 'Spine in background' d) photo of phantom

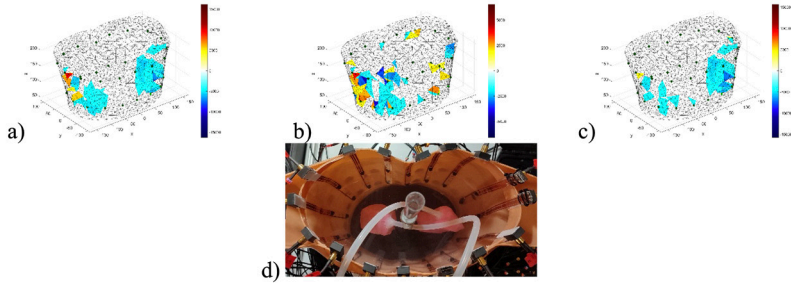


Figure 7. Case reconstructions: Left lung is pumped out, the right lung is filled (a) reference 'Without phantom', (b) reference 'Lungs in the background', (c) reference 'Spine in the background' (d) photo of phantom

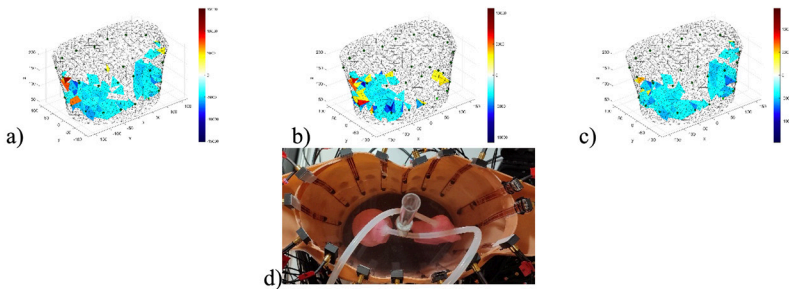


Figure 8. Case reconstructions: Both lungs slightly filled with air (intermediate state) a) reference No phantom, b) reference Lungs in the background, c) reference Spine in the background d) photo of phantom

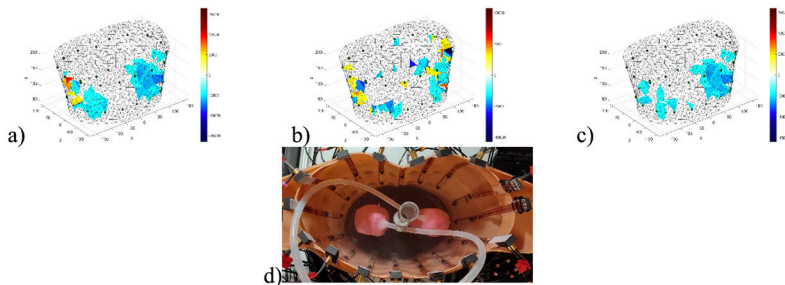


Figure 9: Case reconstructions: Both lungs filled with air (one breath) a) reference 'Without phantom', b) reference 'Lungs in the background', c) reference 'Spine in background' d) photo of phantom

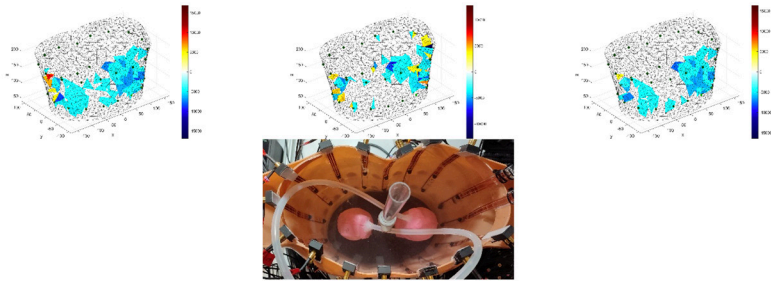
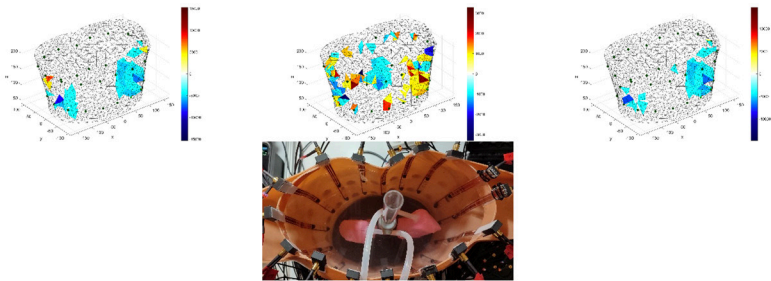


Figure 10. Case reconstructions: Both lungs deflated (complete exhalation) (a) No phantom reference, (b) Background lung reference, (c) Background spine reference (d) photo of phantom



The experiment's results show significant differences in the reconstruction of lung volumes, which are dependent on the state of lung filling. The best reconstruction results were obtained under conditions where no phantom was used ('No phantom'), which allowed the clearest visualization of the lungs without additional background artifacts. When using 'Background Lungs' and 'Background Spine' backgrounds, worse results were observed, especially for the left lung, which was not visible in these settings.

An interesting observation is that the right lung (larger), was better reconstructed in each of the scenarios tested. This observation is as expected, given the asymmetry of human lung anatomy.

The experiment confirmed that the imaging technique used in the study can effectively distinguish between different states of lung filling, which can

be crucial in medical diagnosis, especially in pulmonology studies. The results also indicate the potential need to optimize the reference background to obtain more precise images, especially for the left lung.

CONCLUSIONS

This paper presents a study on the applicability of electroimpedance tomography (EIT) in pulmonary diagnostics. The purpose of the study was to analyze the ability of EIT to reconstruct lung volumes based on different lung filling states that were manipulated in a controlled manner. A series of experiments were performed with varying combinations of filling states of both lungs, illustrated in Figures 2 through 10, showing different scenarios from fully blown to fully inflated lungs. The study was conducted on a phantom reflecting human anatomy. The effects of various reference backgrounds, including 'No phantom', 'Background Lungs', and 'Background Spine', were investigated. Analysis showed that the best image reconstruction quality was achieved without a phantom ('No phantom'), resulting in the clearest visualizations of the lungs. Reduced imaging quality was noted in the 'Background Lungs' and 'Background Spine' backgrounds, especially for the left lung, which was not visible. The experiments confirmed that the larger right lung was systematically better reconstructed regardless of the reference background used.

The paper also emphasizes the importance of using realistic phantom models replicating natural anatomical conditions. The torso phantom designed for the experiment allowed simulations of respiration and other physiological processes affecting EIT results. In conclusion, the study's results indicate that electroimpedance tomography has significant potential to improve the diagnosis of lung diseases, particularly in measuring lung capacity. Further development of this technique, particularly optimization of the reference background and processing algorithms, could help improve the precision and reliability of diagnosis while offering a safe and comfortable testing method for patients.

REFERENCES

- Banasiak, R., Wajman, R., Jaworski, T., Fiderek, P., Fidos, H., Nowakowski, J., Sankowski, D. (2014). Study on two-phase flow regime visualization and identification using 3D electrical capacitance tomography and fuzzy-logic classification. *Int. J. Multiph. Flow*, 58, 1–14.
- Bangti, J., Maass, P. (2012). An Analysis of Electrical Impedance Tomography with Applications to Tikhonov Regularization. *ESAIM COCV*, 18, 1027–1048.
- Berowski, P., Filipowicz, S.F., Sikora, J., Wójtowicz, S. (2005). It is determining location of moisture area of the wall by 3D electrical impedance tomography. In *Proceedings of the 4th World Congress in Industrial Process Tomography*, Aizu, Japan, 5–8 September, pp. 214–219.
- Garbaa, H., Jackowska-Strumiłło, L., Grudzień, K., Romanowski, A. (2016). Application of Electrical Capacitance Tomography and Artificial Neural Networks to Rapid Estimation of Cylindrical Shape Parameters of Industrial Flow Structure. *Arch. Electr. Eng.* 65, 657–669.
- Kania, K., Mazurek, M., Rymarczyk, T. (2022). Application of finite difference method for measurement simulation in ultrasound transmission tomography. *Applied Computer Science*, 18(2), 101–109.
- Kak, A.C., Slaney, M. (1999). *Principles of Computerized Tomographic Imaging*, IEEE Press: New York, NY, USA.
- Kłowski, G., Hoła, A., Rymarczyk, T., Skowron, Ł., Wołowicz, T., Kowalski, M. (2021). The Concept of Using LSTM to Detect Moisture in Brick Walls by Means of Electrical Impedance Tomography. *Energies*, 14, 7617.
- Kłowski, G., Rymarczyk, T., Gola, A. (2018). Increasing the Reliability of Flood Embankments with Neural Imaging Method. *Appl. Sci.* 8, 1457.
- Kłowski, G., Rymarczyk, T., Niderla, K., Rzemieniak, M., Dmowski, A., Maj, M. (2021). Comparison of Machine Learning Methods for Image Reconstruction Using the LSTM Classifier in Industrial Electrical Tomography. *Energies*, 14, 7269.
- Kryszyn, J., Smolik, W. (2017). Toolbox for 3D modelling and image reconstruction in electrical capacitance tomography. *Inform. Control. Meas. Econ. Environ. Prot.* 7, 137–145.
- Kryszyn, J., Wanta, D.M., Smolik, W.T. (2017). Gain Adjustment for Signal-to-Noise Ratio Improvement in Electrical Capacitance Tomography System EVT4. *IEEE Sens. J.* 17, 8107–8116.
- Majchrowicz, M., Kapusta, P., Jackowska-Strumiłło, L., Sankowski, D. (2017). Acceleration of image reconstruction process in the electrical capacitance tomography 3D in heterogeneous, multi-GPU system. *Inform. Control. Meas. Econ. Environ. Prot.*, 7, 37–41.
- Mansouri S, Alharbi Y, Haddad F, Chabcoub S, Alshrouf A, Abd-Elghany AA. (2021). Electrical Impedance Tomography – Recent Applications and Developments. *J Electr Bioimpedance*. 20,12(1):50-62. doi: 10.2478/joeb-2021-0007

- Mikulka, J. (2015). GPU-Accelerated Reconstruction of T2 Maps in Magnetic Resonance Imaging. *Meas. Sci. Rev.* 4, 210–218.
- Mojabi, P., Vetri, J.L. (2016). Development of an ultrasound tomography system: Preliminary results. *J. Acoust. Soc. Am.*, 140, 3419.
- Morigi, M.P., Albertin, (2022). F. X-ray Digital Radiography and Computed Tomography. *J. Imaging*, 8, 119.
- Omeh, DJ., Shlofmitz, E. (2023). Angiography. In: *StatPearls* [Internet]. Treasure Island (FL): StatPearls Publishing, 2024 Jan–. PMID: 32491409.
- Przysucha, B., Rymarczyk, T., Wójcik, D., Woś, M., Vejar, A. (2020). Improving the Dependability of the ECG Signal for Classification of Heart Diseases. In *Proceedings of the 50th Annual IEEE-IFIP International Conference on Dependable Systems and Networks-Supplemental Volume (DSN-S)*, Valencia, Spain, 2–29, 63–64.
- Rymarczyk, T., Kłosowski, G. (2019). Innovative methods of neural reconstruction for tomographic images in maintenance of tank industrial reactors. *Ekspluat. Niezawodn. Maint. Reliab.*, 21, 261–267.
- Rymarczyk, T., Kłosowski, G. (2019). The use of elastic net and neural networks in industrial process tomography. *Przegląd Elektrotechniczny*, 1, 61–64.
- Rymarczyk, T., Kłosowski, G., Hoła, A., Sikora, J., Wołowiec, T., Tchórzewski, P., Skowron, S. (2021). Comparison of Machine Learning Methods in Electrical Tomography for Detecting Moisture in Building Walls. *Energies*, 14, 2777.
- Rymarczyk, T., Kłosowski, G., Kozłowski, E. (2018) A Non-Destructive System Based on Electrical Tomography and Machine Learning to Analyze the Moisture of Buildings. *Sensors*, 18, 2285.
- Rymarczyk, T., Niderla, K., Kozłowski, E., Król, K., Wyrwiz, J.M., Skrzypek-Ahmed, S., Gołabek, P. (2021). Logistic Regression with Wave Preprocessing to Solve Inverse Problem in Industrial Tomography for Technological Process Control. *Energies*, 14, 8116.
- Rymarczyk, T., Król, K., Kozłowski, E., Wołowiec, T. (2021) Cholewa-Wiktor, M., Bednarczuk, P. Application of Electrical Tomography Imaging Using Machine Learning Methods for the Monitoring of Flood Embankments Leaks. *Energies*, 14, 8081.
- Teh JL, Shabbir A, Yuen S, So JB. (2020). Recent advances in diagnostic upper endoscopy. *World J Gastroenterol.* 28,26(4):433-447. doi: 10.3748/wjg.v26.i4.433. PMID: 32063692, PMCID: PMC7002908
- Wang, F., Marashdeh, Q., Fan, L.S., Warsito, W. (2010) Electrical Capacitance Volume Tomography: Design and Applications. *Sensors*, 10, 1890–1917.
- Wajman, R., Fiderek, P., Fidos, H., Jaworski, T., Nowakowski, J., Sankowski, D., Banasiak, R. (2013). Metrological evaluation of a 3D electrical capacitance tomography measurement system for two-phase flow fraction determination. *Meas. Sci. Technol.*, 24, 065302.
- Wislin, J., Malik, B., Borup, D., Pirshafiey, N., John Klock, J. (2020). Full wave 3D inverse scattering transmission ultrasound tomography in the presence of high contrast. *Sci. Rep.*, 10, 20166.

- Zywica, A.R., Ziolkowski, M., Gratkowski, S. (2020). Detailed Analytical Approach to Solve the Magnetoacoustic Tomography with Magnetic Induction (MAT-MI) Problem for Three-Layer Objects. *Energies*, 13, 6515.
- Xi, Y., Qiao, Z., Wang, W., Niu, L. (2020). Study of CT image reconstruction algorithm based on high order total variation. *Optik*, 204, 163814.